

Article

Enhancement of HDO Activity of MoP/SiO₂ Catalyst in Physical Mixture with Alumina or Zeolites

Ivan V. Shamanaev ^{*}, Irina V. Deliy , Evgeny Yu. Gerasimov , Vera P. Pakharukova and Galina A. Bukhtiyarova

Boreskov Institute of Catalysis, Lavrentiev Ave. 5, 630090 Novosibirsk, Russia; delij@catalysis.ru (I.V.D.); gerasimov@catalysis.ru (E.Y.G.); verapakharukova@yandex.ru (V.P.P.); gab@catalysis.ru (G.A.B.)

* Correspondence: i.v.shamanaev@catalysis.ru; Tel.: +7-383-326-9410; Fax: +7-383-330-8056

Received: 21 November 2019; Accepted: 24 December 2019; Published: 31 December 2019



Abstract: Catalytic properties of physical mixture of MoP/SiO₂ catalyst with SiC, γ -Al₂O₃, SAPO-11 and zeolite β have been compared in hydrodeoxygenation of methyl palmitate (MP). MoP/SiO₂ catalyst (11.5 wt% of Mo, Mo/P = 1) was synthesized using TPR method and characterized with N₂ physisorption, elemental analysis, H₂-TPR, XRD and TEM. Trickle-bed reactor was used for catalytic properties investigation at hydrogen pressure of 3 MPa, and 290 °C. The conversions of MP and overall oxygen-containing compounds have been increased significantly (from 59 to about 100%) when γ -Al₂O₃ or zeolite materials were used instead of inert SiC. MP can be converted to palmitic acid through acid-catalyzed hydrolysis along with metal-catalyzed hydrogenolysis, and as a consequence the addition of material possessing acid sites to MoP/SiO₂ catalyst could lead to acceleration of MP hydrodeoxygenation through acid-catalyzed reactions. Isomerization and cracking of alkane were observed over the physical mixture of MoP/SiO₂ with zeolites, but the selectivity of MP conversion through the HDO reaction route is remained on the high level exceeding 90%.

Keywords: molybdenum phosphide; hydrodeoxygenation; methyl palmitate; isomerization

1. Introduction

In the last decade, the research efforts in the transportation fuels production from renewable sources have grown due to environmental issues and limitation of oil reserves [1–4]. One of the versatile and already commercial routes to produce diesel and aviation fuels is hydrodeoxygenation of triglyceride-containing feedstock, including animal fats, waste frying oils, non-edible vegetable oils and so on [5,6]. Oxygen removal from triglyceride molecules includes several alternative routes [7–9]: hydrodeoxygenation (HDO) or decarboxylation/decarbonylation (HDeCO_x). The HDO pathway results in alkanes with the same numbers of carbon atoms in the chain and molecules of water, while HDeCO_x reactions give CO_x molecules and alkanes with the reduced carbon chains [7]. The HDO reaction route is more attractive in terms of atom economy, greenhouse gases production and hydrogen recycle [10,11]. Thus, the current research issue is the design of the catalysts with high activity and high selectivity towards HDO pathway.

Sulfided Ni(Co)Mo/Al₂O₃ catalysts are widely used and studied in triglycerides and esters hydrodeoxygenation [5–7,12–15], but the necessity of the sulfiding agent feeding to save the catalyst in sulfide state stimulate the development of new catalytic systems containing supported metal Ni [16–21], base metal carbides [22–24], nitrides [25] or phosphides [26–35]. Among them, transition metal phosphide catalysts demonstrate promising catalytic properties in hydrodeoxygenation of fatty acids or alkyl esters [26,28,30,32,36], vegetable oils [33], co-processing of renewable oils with petroleum products [37]. The activity of silica-supported catalysts in the HDO of methyl laurate is decreased in the following order [26]: Ni₂P > MoP > CoP–Co₂P > WP > Fe₂P–FeP.

Nevertheless, the high selectivity of MoP-based catalysts in the conversion of aliphatic oxygenates through the HDO route [26] makes MoP/SiO₂ the system of choice from the consideration of carbon atom economy and effluent gases composition, because carbon oxides make difficult purification of circulating hydrogen.

It was reported that acid sites can affect appreciably the HDO of aliphatic esters [26,29,38–46]. The authors of [26,29,39,40] have proposed, that Brønsted acidic sites of silica-supported nickel phosphide catalysts participate in the reaction of carboxylic ester to carboxylic acid. Also, the rate of ethyl stearate HDO over Ru/TiO₂ catalyst was increased when the catalyst was mixed with the grains of γ -Al₂O₃ [41]. The synergetic effect of Ni₂P/SiO₂ and γ -Al₂O₃ physical mixture was observed in methyl palmitate HDO resulting in the enhancement of methyl palmitate conversion over Ni₂P/SiO₂ catalyst after mixing it with alumina grains [42]. It was observed that Ni₂P catalyst supported on γ -Al₂O₃ exhibits higher conversion of methyl palmitate HDO in comparison with silica-supported one, though both catalysts contain Ni₂P nanoparticles with close mean particle size and nearly the same nickel content [43]. The authors [42,43] proposed that the acid sites of the alumina increase the reaction rate of methyl palmitate hydrolysis, that enhance the methyl palmitate conversion. The assumption was made earlier [44,45], that the Lewis acid sites of the support enhance the rate of hydrolysis of aliphatic esters over alumina-supported sulfide catalysts.

The above examples of activity enhancement in the presence of acidic material allowed us to suggest that the replacement of silica support with the alumina may increase the catalytic activity of MoP catalyst in methyl palmitate HDO without reducing selectivity. The synthesis of supported MoP/ γ -Al₂O₃ catalysts is sophisticated task due to interaction between alumina surface and phosphate groups that makes the reduction difficult and prevents the formation of MoP nanoparticles on alumina support [47–49]. Up to now, the silica-supported MoP catalysts have been studied in the HDO reactions, due to relatively easy reduction of phosphate groups that makes possible the formation of highly dispersed MoP phase on silica support [26,50].

The goal of the current study is the investigation of the catalytic properties of mechanical mixtures of MoP/SiO₂ catalyst and materials with different acidity (SiC, γ -Al₂O₃, SAPO-11 and zeolite β) in methyl palmitate hydrodeoxygenation as the representative model component of triglyceride-based feedstock.

2. Results and Discussion

2.1. Catalyst Characterization

Physicochemical properties of MoP/SiO₂, prepared using phosphate and phosphite precursors by TPR are shown in Table 1. MoP_A was prepared using ammonium paramolybdate and ammonium phosphate, MoP_I was prepared using ammonium paramolybdate and phosphorous acid. MoP is a bulk sample, prepared for comparison and XRD analysis. Initial Mo/P molar ratio in impregnating solution was 1. This ratio is usually used to prepare MoP catalysts [26,51] and the samples with this ratio were shown to be more active in hydrotreating reactions [52]. After reduction Mo/P ratio is slightly decreased to 0.91 for MoP_A and MoP and to 0.83 for MoP_I (Table 1). This can be due to Mo losses at impregnation step. Mo/P ratio determined from EDX data differ slightly from the chemical analysis results, but still remains close to Mo/P = 1.

Table 1. Physicochemical properties of SiO₂, MoP/SiO₂ and MoP samples.

Sample	Mo, wt%	P, wt%	Mo/P Molar Ratio in Reduced Catalyst	Mo/P EDX	S _{BET} , m ² /g	D _{pore} , nm	D _{TEM} , nm	XRD Phase	D _{XRD} , nm
SiO ₂	–	–	–	–	300	10.6	–	–	–
MoP_A	11.5	4.0	0.91	1.02	178	10.4	1.4	amorphous phase	–
MoP_I	11.5	4.3	0.83	0.97	235	7.9	2.0	amorphous phase	–
MoP	51.7	18.4	0.91	1.17	211	2.0	–	MoP	12

Initial SiO₂ support has S_{BET} = 300 m²/g and D_{pore} = 10.6 nm. MoP_A and MoP_I have decreased value of S_{BET} and D_{pore} in comparison with the silica support. Both active component and unreduced phosphate groups can block pores and decrease S_{BET}. Bulk MoP has quite high area due to presence of large quantities of citric acid in the precursor, which are transformed to carbon after reduction.

The precursors and PO_x/SiO₂ samples were investigated by H₂-TPR (Figure 1). There are two peaks for the bulk MoP precursor: at 490 and at 720 °C. The first corresponds to Mo⁺⁶ → Mo⁺⁴ reduction, the second corresponds to Mo⁺⁴ → Mo^{δ+} and P⁺⁵ → P^{δ-} phosphide formation. Reduction of phosphates in PO_x/SiO₂ sample occurs at higher temperatures (> 750 °C, Figure 1). H₂-TPR of MoP_A and MoP_I precursors have the maximums at the temperatures similar to the reduction temperature of bulk MoP. H₂-TPR shows that precursor nature does not influence the temperatures of reduction of silica-supported MoP precursors. It was shown that in the case of Ni-based phosphide catalysts during H₂-TPR of phosphite precursors the additional amount of hydrogen is produced, which is detected in H₂-TPR curves [40,43]. For the Mo-phosphide precursors there is only slight difference between H₂-TPR curves of MoP_A and MoP_I precursors (Figure 1). This can be attributed to oxidation of HPO₃²⁻ by paramolybdate after impregnation:

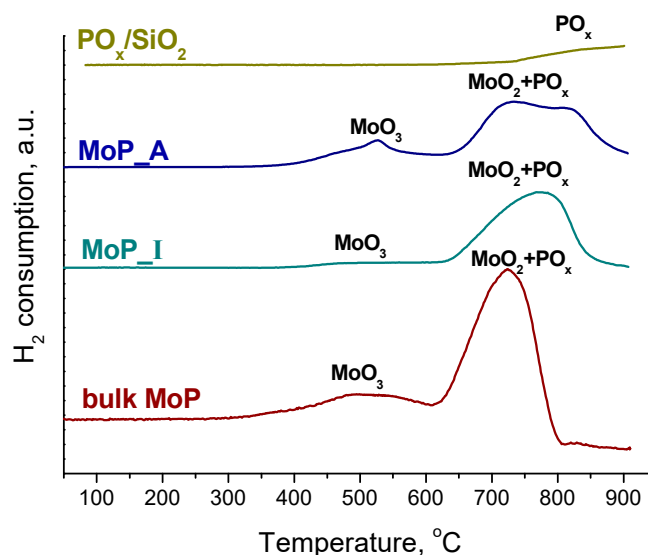
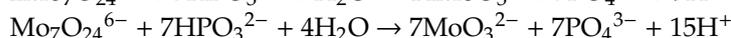


Figure 1. H₂-TPR curves of PO_x/SiO₂, supported MoP_A, MoP_I and bulk MoP oxide precursors.



These reactions are visible, because presence of Mo(IV/V) species gives the characteristic blue color of the catalysts. Moreover, the reduction peak of MoO₃ in H₂-TPR of MoP_I sample is almost invisible (Figure 1), which corresponds to the presence of Mo, preferably in Mo (IV/V) states.

The calculated consumption of H₂ during MoP_A reduction is 1.1 mmol/g, while the MoP_I consumes 0.80 mmol/g. This difference can be explained by the different states of Mo species.

XRD analysis of unreduced bulk MoP precursor did not show presence of any crystal phases (Figure 2), only increased intensity at low 2θ angles, which corresponds to amorphous carbon residues. XRD pattern of reduced bulk MoP sample include well defined maximums, corresponding to MoP phase (PDF № 24-0771). This pattern also has some amorphous phase corresponding to an increased base line in a 2θ range of 35–40°. D_{XRD} of MoP particles is 12 nm (Table 1). In supported MoP_A and MoP_I samples, there were broad signals of SiO₂ at ~20°; low-intensive broadening is also observed in the range of 35–45° that can be due to highly dispersed MoP (<3 nm) nanoparticles.

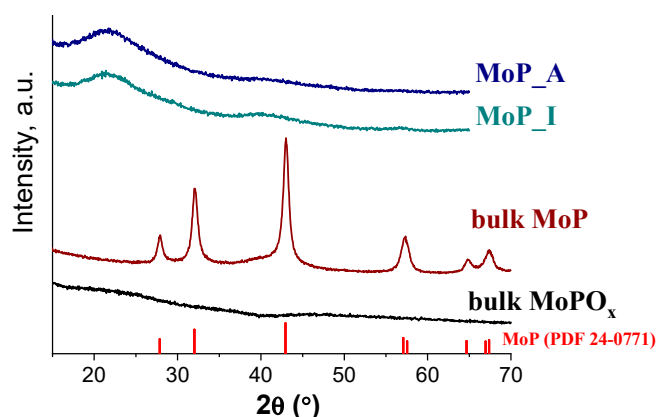


Figure 2. XRD of reduced MoP_A, MoP_I and bulk MoP samples and unreduced MoP precursor.

Figure 3 shows images of TEM analysis of MoP_A, MoP_I and bulk MoP samples. Size distributions of MoP particles are shown for MoP_A and MoP_I samples. Supported MoP_A and MoP_I samples have quite small particles (1.4 and 2.0 nm correspondingly, Table 1) and narrow particle size distributions. MoP sample has particles of 10–50 nm; therefore, there is no particle size distribution on Figure 3 for this sample.

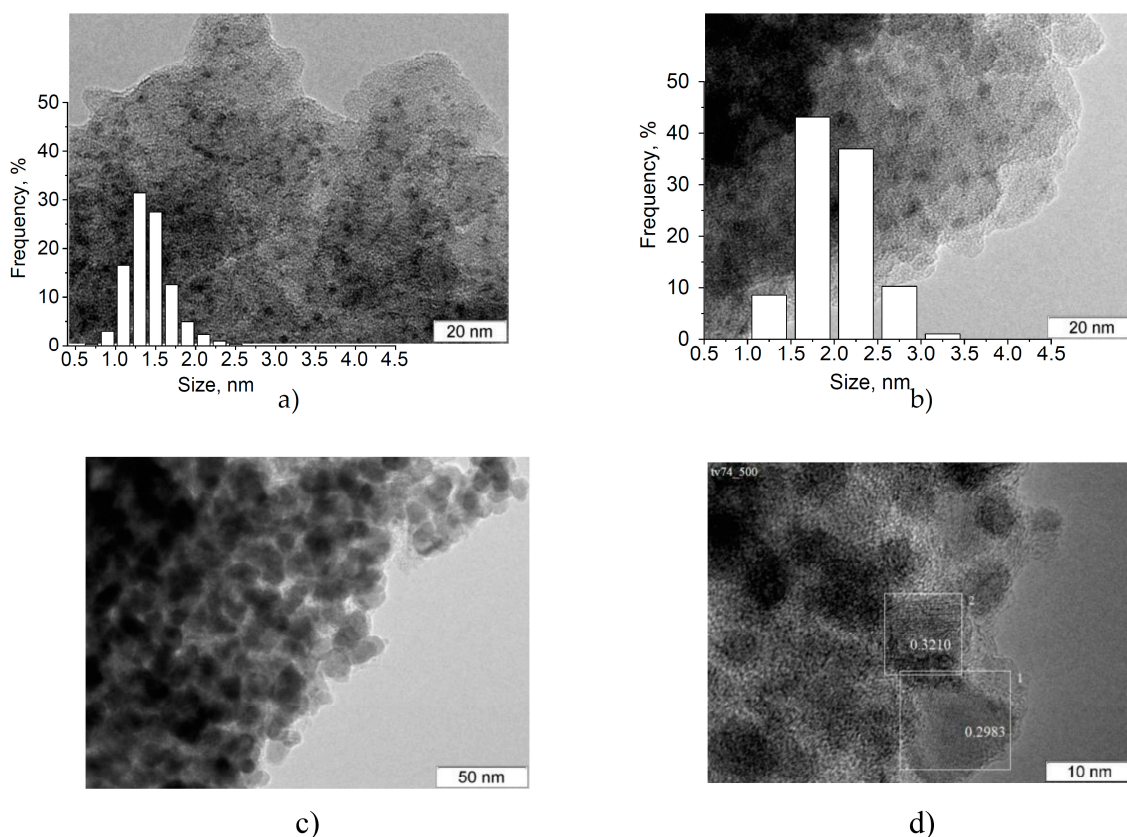


Figure 3. Images of TEM MoP_A (a), MoP_I (b), bulk MoP (c,d).

In preliminary MP HDO experiments ($LHSV = 60 \text{ h}^{-1}$, $T = 290 \text{ }^\circ\text{C}$, $P_{\text{H}_2} = 3 \text{ MPa}$, $\text{H}_2/\text{feed} = 600 \text{ cm}^3/\text{cm}^3$) 59 and 60% MP conversion were obtained over MoP_A and MoP_I, respectively. MoP_A sample was used for catalytic experiments with different diluters.

The diluters used for catalytic experiments in this work were SiC, γ -Al₂O₃, SAPO-11 and zeolite β (Table 2). XRD analysis proved corresponding crystal structures for these materials (Figure S1 in Supporting Information).

Table 2. Physicochemical properties of the diluters.

Diluter	S _{BET} , m ² /g	V _{pore} , cm ³ /g	D _{pore} , nm	NH ₃ -TPD, 10 ⁻³ mol/g
SiC	1	–	–	–
γ -Al ₂ O ₃	235	0.79	13.4	0.421
SAPO-11	295	0.26	3.5	1.11
zeolite β	609	0.49	3.2	1.92

Unlike SiC, an inert material with extremely low S_{BET} (1 m²/g), γ -Al₂O₃, SAPO-11 and zeolite β have developed textural structures (Table 2). The acidity of these materials, in accordance with NH₃-TPD data, is decreased in the following order: zeolite β > SAPO-11 > γ -Al₂O₃ (Table 2).

Zeolite β is characterized by Brønsted acid sites and three-dimensional system of channels, with sizes of 0.56 × 0.56 and 0.66 × 0.67 nm [53]. SAPO-11 has one-dimensional system of channels with size of 0.40 × 0.65 nm. SAPO-11 is a mesoporous structure, which has Brønsted acid sites of middle strength [54].

2.2. MP HDO Results

Catalytic properties of physical mixtures of MoP/SiO₂ with SiC, γ -Al₂O₃, SAPO-11 or zeolite β were investigated in MP HDO at T = 290 °C, P_{H₂} = 3 MPa, H₂/feed = 600 cm³/cm³, LHSV = 60 or 10 h⁻¹, using 0.4 or 1.4 g of catalyst and volume ratio of V_{cat}:V_{diluter} = 1:10.5 or 1:1.5. Stable conversion as a function of time on stream was obtained for all tested systems (Figure S2 in Supporting Information). The results of comparative study of these systems in the methyl palmitate HDO are presented on Figure 4, which displays the values of MP conversion (X_{MP}) and oxygen conversion (X_O). MoP/SiO₂ sample diluted with inert SiC grains displays the lowest X_{MP} (59%) and X_O (55%) values, whereas X_{MP} and X_O data for systems containing γ -Al₂O₃, zeolite β and SAPO-11 are higher than 90%. It is well known that HDO of fatty acid esters includes consecutive and parallel reactions: hydrogenolysis of C–O (HDO) and C–C (HDeCO_x) bonds, hydrolysis of ester, hydrogenation of double bounds, dehydration of alcohols and esterification of acids, which occur over metal and acid active sites of catalysts, supports and diluters [26,42,55]. In particular, MP can be transformed at metal centers through hydrogenolysis to acid or aldehyde, or via acid-catalyzed hydrolysis to acid [56]. Thus, the higher conversions of MP over MoP/SiO₂ catalyst in the presence of Al₂O₃, SAPO-11 or zeolite β can be explained by the higher rate of methyl palmitate hydrolysis, which is favored by the acid sites of these materials.

The main HDO product over MoP/SiO₂–SiC and MoP/SiO₂– γ -Al₂O₃ is hexadecane at 100% conversion of MP; the selectivity of MP conversion through the HDO pathway exceeds 96% (Figure 5). Thus, the use of γ -Al₂O₃ instead of SiC in the mixture with MoP/SiO₂ increases the MP conversion, but has minor impact on the product distribution. The dilution of MoP/SiO₂ with the same amount of SAPO-11 or zeolite β instead of SiC decreases the selectivity of C₁₆ alkane formation in the course of MP HDO and increases the quantity of iso-C₁₆, iso-C₁₅ and C₆–C₁₄ hydrocarbons among the liquid products. Especially increased formation of hydrocarbons with ≤14 carbon atoms in the hydrocarbon chains is observed over MoP/SiO₂–zeolite β catalytic system. Apparently, Brønsted acid sites in MoP/SiO₂–SAPO-11 and MoP/SiO₂–zeolite β result in partial cracking and structural isomerization of linear C₁₅ and C₁₆ hydrocarbons, which are formed in the HDO reaction of the ester. In these cases, the secondary reactions of the alkanes that are formed in MP HDO make it unattainable to calculate selectivities of HDO and HDeCO_x pathways using the results of liquid phase analysis. To estimate the effect of SAPO-11 and zeolite β on the selectivity of MP conversion the amounts of carbon oxides were compared for MoP/SiO₂–SiC, MoP/SiO₂–SAPO-11 and MoP/SiO₂–zeolite β (Figure 6). The results obtained let us see that the use of MoP/SiO₂–SAPO-11 and MoP/SiO₂–zeolite β induces only negligible

increase in the amounts of carbon oxides in the gas phase in comparison with MoP/SiO₂–SiC system. Appreciable amounts of light hydrocarbons with the carbon number ≤5 were detected in the gas-phase products of MP HDO over MoP/SiO₂–zeolite β that is the evidence of alkane overcracking in the presence of zeolite β.

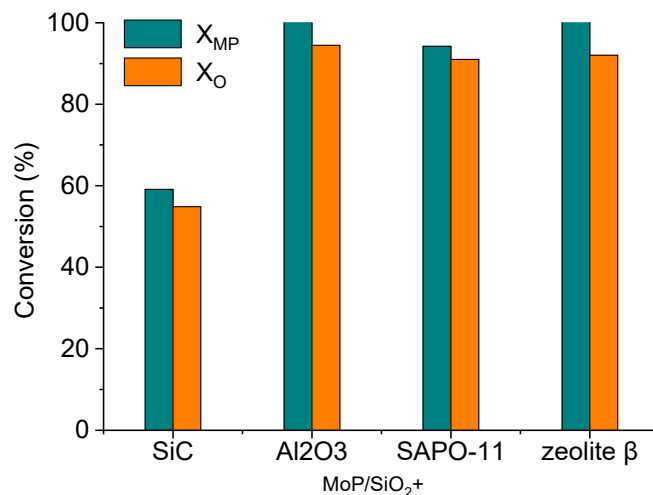


Figure 4. MP and O conversion in MP HDO over MoP/SiO₂ catalyst diluted with different materials. $V_{\text{cat}} = 0.4 \text{ cm}^3$, LHSV = 60 h⁻¹, T = 290 °C, $P_{\text{H}_2} = 3 \text{ MPa}$, $\text{H}_2/\text{feed} = 600 \text{ cm}^3/\text{cm}^3$.

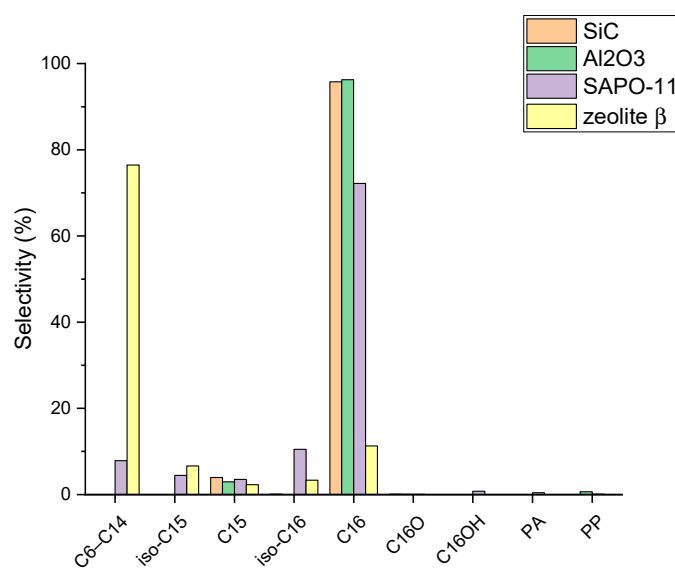


Figure 5. Selectivities of MP HDO products over MoP/SiO₂ catalyst diluted with different materials ($X_{\text{MP}} = 100\%$). C₁₆O—hexadecanal, C₁₆OH—hexadecanol, PA—palmitic acid, PP—palmityl palmitate. $V_{\text{cat}} = 1.8 \text{ cm}^3$, LHSV = 10 h⁻¹, T = 290 °C, $P_{\text{H}_2} = 3 \text{ MPa}$, $\text{H}_2/\text{feed} = 600 \text{ cm}^3/\text{cm}^3$.

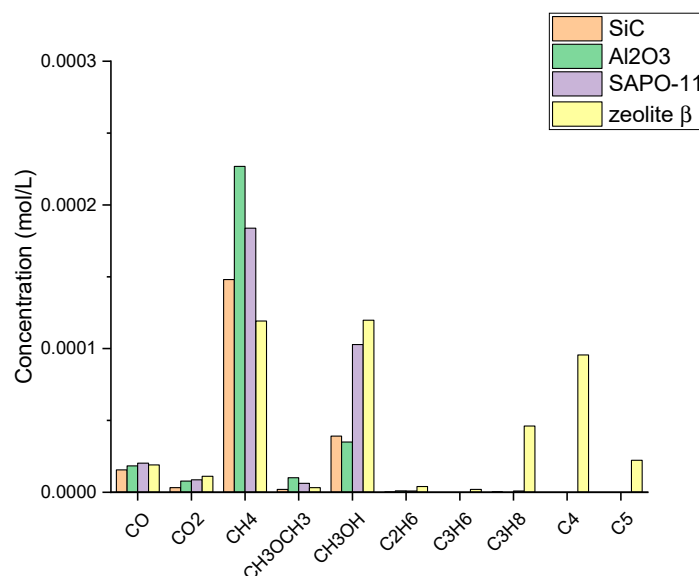


Figure 6. Concentration of gas-phase products of MP HDO over MoP/SiO₂ catalyst diluted with different materials ($X_{MP} = 100\%$). $V_{cat} = 1.8 \text{ cm}^3$, $LHSV = 10 \text{ h}^{-1}$, $T = 290 \text{ }^\circ\text{C}$, $P_{H_2} = 3 \text{ MPa}$, $H_2/\text{feed} = 600 \text{ cm}^3/\text{cm}^3$.

The above results show that the use of the MoP/SiO₂ catalyst in the mixtures with acidic materials, like γ -Al₂O₃, SAPO-11 and zeolite β improves the catalytic activity of MoP catalyst in the hydrodeoxygenation of MP without reducing selectivity through HDO pathway. MoP/SiO₂- γ -Al₂O₃ system gives hexadecane with the selectivity up to 96%, while MoP/SiO₂-SAPO-11 produces iso-alkane and some amount of C₆-C₁₄ hydrocarbons. Therefore, MoP catalysts on SAPO-11 are perspective in one-pot HDO/hydroisomerization of aliphatic esters.

3. Materials and Methods

3.1. Catalysts Preparation

Commercial silica “KSKG” ($S_{BET} = 300 \text{ m}^2/\text{g}$, $V_{pore} = 0.80 \text{ cm}^3/\text{g}$, $D_{pore} = 10.6 \text{ nm}$) was obtained from ChromAnalit (Moscow, Russia), it was used as support material. Commercial SiC (Chelyabinsk Plant of Abrasive Materials, Chelyabinsk, Russia), alumina “IKGO-1” (γ -Al₂O₃, Promkataliz, Ryazan, Russia), zeolite β in H form (Angarsk catalyst and organic synthesis plant, Angarsk, Russia), SAPO-11 (Zeolyst International, Conshohocken, PA, USA) were utilized as diluters. Before catalysts preparation and experiments silica and alumina were dried (at 110 °C, 7 h) and calcined (at 500 °C, 4 h). Afterwards the materials were crushed using mortar and pestle, and sieved to obtain granules with size of 0.25–0.50 mm.

Preparation method of MoP/SiO₂ samples

Incipient wetness impregnation method was used to prepare precursors of MoP/SiO₂ samples. Mo/P molar ratio in impregnation water solution was taken equal 1 (Mo content ~11.5 wt%). The label MoP_A was chosen for the MoP/SiO₂ sample, which was prepared from phosphate solution, the label MoP_I—for the MoP/SiO₂ sample, which was prepared from phosphite solution.

Phosphate method (MoP_A). To synthesis samples using this technique 2.357 g of (NH₄)₂HPO₄ (Alfa Aesar, Kandel, Germany) and 3.151 g of (NH₄)₆Mo₇O₂₄·4H₂O (Reakhim, Moscow, Russia) were dissolved under stirring in distilled water. Subsequently the support (8.5 g SiO₂) was impregnated by this solution. After drying on air overnight (at room temperature) the precursors were dried for 4 h at 110 °C. Calcination of the dried samples was carried out at 500 °C for 4 h, and reduction of the calcined samples (TPR) was performed in H₂ flow (100 mL/(min·g)). TPR has the following program: heating to 370 °C (with the rate of 3 °C/min), heating to 650 °C (with the rate of 1 °C/min), keeping the samples

at 650 °C (for 1 h). Passivation of the reduced samples (to prevent oxidation on air atmosphere) was carried out at room temperature in 1 vol% O₂/He (at 40 mL/(min·g) for 2 h).

Phosphite method (MoP_I). First, silica support (8.5 g) was impregnated with aqueous solution containing 3.151 g of (NH₄)₆Mo₇O₂₄·4H₂O and 1.464 g of H₃PO₃. Then, after drying overnight and subsequently at 80 °C (for 24 h), the samples were reduced (TPR) in H₂ flow (100 mL/(min·g)). TPR was carried as follows: heating to 650 °C (with the rate of 1 °C/min), keeping at 650 (for 1 h). The same passivation technique was carried out for MoP_I samples as in case of MoP_A samples.

PO_x/SiO₂ sample. SiO₂ (5 g) was impregnated by the solution of 2.357 g of (NH₄)₂HPO₄ in distilled water. Drying was performed at room temperature overnight and at 110 °C (for 4 h). After calcination at 500 °C (for 4 h), the precursor was reduced and passivated according the same TPR and passivation programs as for MoP_A and MoP_I precursors.

Bulk MoP reference sample preparation method. The bulk molybdenum phosphide sample (bulk MoP) was prepared as follows: to the water solution of (NH₄)₂HPO₄ was added water solution of (NH₄)₆Mo₇O₂₄. The Mo/P initial molar ratio was equal to 1. After evaporation of the water, the obtained sample was dried at 87 °C (for 48 h) and then at 124 °C (for 24 h). Calcination of the sample was performed at 500 °C (for 5 h). Afterwards, TPR was carried out (at H₂ flow of 150 mL/(min·g)): heating to 650 °C (with the rate of 1 °C/min), keeping at 650 °C (for 1 h). The obtained bulk sample was passivated in flow of 1 vol.% O₂/He (80 mL/(min·g), for 3 h).

3.2. Catalysts Characterization

Nitrogen physisorption was used to determine textural characteristics of the MoP, MoP/SiO₂ and diluters. It was carried out at 77 K on ASAP 2400 instrument (USA).

Inductively coupled plasma atomic emission spectroscopy (ICP-AES) was used to perform elemental analysis of the MoP and MoP/SiO₂ samples. ICP-AES was carried out on Optima 4300 DV (Perkin Elmer, Villebon-sur-Yvette, France).

Bruker D8 Advance X-ray diffractometer (Bruker, Bremen, Germany) was used to carry out XRD analysis. CuK_α radiation (with $\lambda = 1.5418 \text{ \AA}$) was used, and 2 θ scanning range was from 10 to 70. To determine crystal phases JCPDS database was used [57]. Scherrer equation was used to calculate average crystallite size (D_{XRD}).

Transmission electron microscope JEM-2010 (JEOL, Tokyo, Japan) was used to obtain high resolution transmission electron microscopy (TEM) images. The accelerating voltage and resolution were 200 kV and 0.14 nm correspondingly. EDX spectrometer was used to analyze elemental composition.

H₂ temperature-programmed reduction (H₂-TPR) was performed to determine reduction temperatures of the prepared samples. The sample mass was about 0.10 g, it was heated in 10 vol.% H₂/Ar (60 mL/min, with rate of 10 °C/min) from 80 °C to 900 °C. Thermal conductivity detector (TCD) was used to determine H₂ consumption.

3.3. Experimental Setup and Procedure

Methyl palmitate (hexadecanoic acid methyl ester, $\geq 97\%$), *n*-dodecane ($\geq 99\%$) and *n*-octane ($\geq 99.5\%$) were obtained from Sigma-Aldrich (St. Louis, MO, USA), Acros Organics (New Jersey, NJ, USA) and Kriokhrom (Saint Petersburg, Russia), correspondingly.

A trickle-bed reactor was used to evaluate catalytic activity of the prepared MoP catalysts in methyl palmitate HDO (Figure S3 in Supporting Information). The reaction conditions: T = 290 °C, P_{H₂} = 3.0 MPa, volume ratio H₂/feed = 600, LHSV = 60 or 10 h⁻¹. The liquid feed consisted of: 10 wt% of methyl palmitate, 0.5 wt% of *n*-octane (internal standard), the rest is *n*-dodecane. The catalysts particles were diluted with SiC, Al₂O₃, SAPO-11 or zeolite β (0.2–0.3 mm) in a ratio 1:10.5 or 1:1.5, placed in the catalytic reactor between. Above and under the catalytic layer there were SiC layers. Before methyl palmitate HDO experiments reduction of the catalyst precursors was performed in situ by TPR technique described earlier in catalysts preparation section. Collecting of liquid product

effluent was carried out hourly until the reaction reaches steady-state. For all experiments time on stream = 8 h (Figure S2 in Supporting Information).

X_{MP} —methyl palmitate conversion was calculated as follows:

$$X_{MP} = \left(1 - \frac{C_{MP}}{C_{MP}^0}\right) \cdot 100\% \quad (1)$$

c_{MP}^0 and c_{MP} (mol/L)—methyl palmitate concentration in the initial feed and in the liquid product correspondingly.

X_O —oxygen-containing compounds conversion was calculated as follows:

$$X_{OCC} = \left(1 - \frac{C_O}{C_O^0}\right) \cdot 100\% \quad (2)$$

c_O^0 and c_O (mol/L)—oxygen concentration in the initial feed and in the liquid product correspondingly.

S_i —selectivity was calculated as follows:

$$S_i = \left(\frac{c_i}{c_{MP}^0 - c_{MP}}\right) \cdot 100\% \quad (3)$$

c_i (mol/L)—concentration of the i th compound in the liquid product.

3.4. Analysis of the Reaction Products

7000 GC/MS Triple QQQ GC System 7890A (Agilent Technologies, Santa Clara, CA, USA) was used to identify HDO products. The GC was equipped with VF-5MS column (length 30 m, inner diameter 0.25 mm, film thickness 0.25 μ m). Quantitative analysis was performed using GC with flame ionization detector (FID, Agilent 6890N, USA) and an HP-1MS column (length 30 m, inner diameter 0.32 mm, film thickness 1.0 μ m). Carbon balance for all experiments was not lower than 97%.

Elemental analyzer Vario EL Cube (Elementar Analysensysteme GmbH, Langensfeld, Germany) was used to determine oxygen content in the liquid reaction mixture.

The concentration of gas-phase products was determined using GC Khromos-1000 with FID (Khromos, Dzerzhinsk, Russia). CO and CO₂ were analyzed after methanation over Pd catalyst.

4. Conclusions

In this work catalytic properties of MoP/SiO₂ catalyst in MP HDO were studied in mechanical mixture with materials having different acidity: SiC, γ -Al₂O₃, SAPO-11 and zeolite β .

A method was chosen for the preparation of SiO₂-supported MoP catalyst. Two samples were prepared using (NH₄)₆Mo₇O₂₄ and different P precursors: (NH₄)₂HPO₄ and H₃PO₃ (MoP_A and MoP_I samples, correspondingly). It was shown that H₂-TPR curves for MoP_A and MoP_I samples are coinciding regardless of P precursor that can be explained by the oxidation of H₃PO₃ in the reaction with ammonium paramolybdate during impregnation and drying of support. The silica-supported MoP catalysts samples were synthesized by reduction (TPR) of the precursors at 650 °C, and according to TEM data, the particle sizes of MoP nanoparticles were 1.4 and 2.0 nm for MoP_A and MoP_I samples, respectively. Both catalysts (MoP_A and MoP_I) display similar activity in the MP hydrodeoxygenation; MoP_A sample (designated as MoP/SiO₂) was chosen for the experiments with different diluters.

The comparative study of MoP/SiO₂-SiC, MoP/SiO₂- γ -Al₂O₃, MoP/SiO₂-SAPO-11 and MoP/SiO₂-zeolite β systems has demonstrated the enhancement of MoP/SiO₂ catalyst activity in MP HDO in mechanical mixtures with alumina, SAPO-11 and zeolite β . The higher conversions of MP over MoP/SiO₂ catalyst in the presence of Al₂O₃, SAPO-11 and zeolite β can be explained by the higher rate of methyl palmitate hydrolysis, which is favored by the acid sites of these materials. The use

of γ - Al_2O_3 , SAPO-11 and zeolite β instead of SiC in the mixture with MoP/SiO₂ increases the MP conversion, but has minor impact on the HDO selectivity. It was shown that selectivities of methyl palmitate conversion through the HDO pathways are nearly the same for the different systems, because the amounts of CO and CO₂ in the gas-phase products differ only slightly. The main HDO product observed in the liquid products of MP HDO over MoP/SiO₂-SiC and MoP/SiO₂- γ -Al₂O₃ is hexadecane; the selectivity of HDO pathway exceeds 96% at 100% of MP conversion. The use of MoP/SiO₂ in the mixture with the SAPO-11 or zeolite β instead of SiC changes the product distribution due to partial cracking and structural isomerization of linear C₁₅ and C₁₆ hydrocarbons, which are formed in HDO reaction of ester. Thus, MoP/SiO₂-SAPO-11 system produces iso-alkane and some amount of C₆-C₁₄ hydrocarbons, while increased formation of hydrocarbons with ≤ 14 carbon atoms in the hydrocarbon chains is observed over MoP/SiO₂-zeolite β catalytic system.

The obtained results show, that the use of the MoP/SiO₂ catalyst in the mixtures with γ -Al₂O₃, SAPO-11 and zeolite β enhances the catalytic activity of MoP catalyst in the hydrodeoxygenation of MP without reducing selectivity through HDO pathway. The product distribution in the liquid phase depends on the dilutor nature. Linear alkanes are produced in the presence of γ -Al₂O₃. SAPO-11 can be considered as the perspective material for the one-pot HDO/hydroisomerization of aliphatic esters.

Supplementary Materials: The following are available online at <http://www.mdpi.com/2073-4344/10/1/45/s1>, Figure S1: XRD patterns of materials used as catalyst diluters, Figure S2: MP conversion vs time on stream for MoP/SiO₂ catalysts diluted with different materials, Figure S3: The scheme of the experimental setup.

Author Contributions: Formal analysis, I.V.S. and I.V.D.; TEM analysis, E.Y.G.; XRD analysis, V.P.P.; writing and the draft preparation, I.V.D., I.V.S. and G.A.B.; reviewing and editing, I.V.D., G.A.B. and I.V.S.; supervision, G.A.B. All authors have read and agreed to the published version of the manuscript.

Funding: This work was supported by Ministry of Science and Higher Education of the Russian Federation (project AAAA-A17-117041710075-0). The authors of the paper are grateful to M.V. Shashkov and V.A. Utkin for analysis and identification of HDO reaction products by GC/MS.

Conflicts of Interest: The authors declare no conflict of interest.

References

1. Choudhary, T.V.; Phillips, C.B. Renewable fuels via catalytic hydrodeoxygenation. *Appl. Catal. A Gen.* **2011**, *397*, 1–12. [[CrossRef](#)]
2. Serrano-Ruiz, J.C.; Ramos-Fernández, E.V.; Sepúlveda-Escribano, A. From biodiesel and bioethanol to liquid hydrocarbonfuels: New hydrotreating and advanced microbial technologies. *Energy Environ. Sci.* **2012**, *5*, 5638–5652. [[CrossRef](#)]
3. Huber, G.W.; Iborra, S.; Corma, A. Synthesis of transportation fuels from biomass: Chemistry, catalysts, and engineering. *Chem. Rev.* **2006**, *106*, 4044–4098. [[CrossRef](#)] [[PubMed](#)]
4. Melero, J.A.; Iglesias, J.; Garcia, A. Biomass as renewable feedstock in standard refinery units. Feasibility, opportunities and challenges. *Energy Environ. Sci.* **2012**, *5*, 7393–7420. [[CrossRef](#)]
5. Khan, S.; Kay Lup, A.N.; Qureshi, K.M.; Abnisa, F.; Wan Daud, W.M.A.; Patah, M.F.A. A review on deoxygenation of triglycerides for jet fuel range hydrocarbons. *J. Anal. Appl. Pyrolysis* **2019**, *140*, 1–24. [[CrossRef](#)]
6. Why, E.S.K.; Ong, H.C.; Lee, H.V.; Gan, Y.Y.; Chen, W.-H.; Chong, C.T. Renewable aviation fuel by advanced hydroprocessing of biomass: Challenges and perspective. *Energy Convers. Manag.* **2019**, *199*, 112015. [[CrossRef](#)]
7. Kubička, D.; Tukač, V. Chemical Engineering for Renewables Conversion. Advances in Chemical Engineering. In *Advances in Chemical Engineering*; Murzin, D.Y., Ed.; Elsevier: Amsterdam, The Netherlands, 2013; Volume 42, pp. 141–194. ISBN 9780123865052.
8. Zharova, P.A.; Chistyakov, A.V.; Shapovalov, S.S.; Pasynskii, A.A.; Tsodikov, M.V. Original Pt-Sn/Al₂O₃ catalyst for selective hydrodeoxygenation of vegetable oils. *Energy* **2019**, *172*, 18–25. [[CrossRef](#)]
9. Kukushkin, R.G.; Reshetnikov, S.I.; Zavarukhin, S.G.; Eletsii, P.M.; Yakovlev, V.A. Kinetics of the Hydrodeoxygenation of Ethyl Ester of Decanoic Acid over the Ni-Cu-Mo/ Al₂O₃ Catalyst. *Catal. Ind.* **2019**, *11*, 191–197. [[CrossRef](#)]

10. Janampelli, S.; Darbha, S. Selective and reusable Pt-WO_x/ Al₂O₃ catalyst for deoxygenation of fatty acids and their esters to diesel-range hydrocarbons. *Catal. Today* **2018**, *309*, 219–226. [[CrossRef](#)]
11. Gosselink, R.W.; Stellwagen, D.R.; Bitter, J.H. Tungsten-Based Catalysts for Selective Deoxygenation. *Angew. Chem. Int. Ed.* **2013**, *52*, 5089–5092. [[CrossRef](#)]
12. Wang, H.; Rogers, K.; Zhang, H.; Li, G.; Pu, J.; Zheng, H.; Lin, H.; Zheng, Y.; Ng, S. The Effects of Catalyst Support and Temperature on the Hydrotreating of Waste Cooking Oil (WCO) over CoMo Sulfided Catalysts. *Catalysts* **2019**, *9*, 689. [[CrossRef](#)]
13. Zhao, X.; Wei, L.; Cheng, S.; Julson, J. Review of Heterogeneous Catalysts for Catalytically Upgrading Vegetable Oils into Hydrocarbon Biofuels. *Catalysts* **2017**, *7*, 83. [[CrossRef](#)]
14. Pinheiro, A.; Dupassieux, N.; Hudebine, D.; Geantet, C. Impact of the Presence of Carbon Monoxide and Carbon Dioxide on Gas Oil Hydrotreatment: Investigation on Liquids from Biomass Cotreatment with Petroleum Cuts. *Energy Fuels* **2011**, *25*, 804–812. [[CrossRef](#)]
15. Philippe, M.; Richard, F.; Hudebine, D.; Brunet, S. Transformation of dibenzothiophenes model molecules over CoMoP/ Al₂O₃ catalyst in the presence of oxygenated compounds. *Appl. Catal. B Environ.* **2013**, *132*, 493–498. [[CrossRef](#)]
16. Liu, S.; Zhu, Q.; Guan, Q.; He, L.; Li, W. Bio-aviation fuel production from hydroprocessing castor oil promoted by the nickel-based bifunctional catalysts. *Bioresour. Technol.* **2015**, *183*, 93–100. [[CrossRef](#)]
17. Li, X.; Luo, X. Preparation of mesoporous activated carbon supported Ni catalyst for deoxygenation of stearic acid into hydrocarbons. *Environ. Prog. Sustain. Energy* **2015**, *34*, 607–612. [[CrossRef](#)]
18. Kukushkin, R.G.; Bulavchenko, O.A.; Kaichev, V.V.; Yakovlev, V.A. Influence of Mo on catalytic activity of Ni-based catalysts in hydrodeoxygenation of esters. *Appl. Catal. B Environ.* **2015**, *163*, 531–538. [[CrossRef](#)]
19. Yakovlev, V.A.; Khromova, S.A.; Sherstyuk, O.V.; Dundich, V.O.; Ermakov, D.Y.; Novopashina, V.M.; Lebedev, M.Y.; Bulavchenko, O.; Parmon, V.N. Development of new catalytic systems for upgraded bio-fuels production from bio-crude-oil and biodiesel. *Catal. Today* **2009**, *144*, 362–366. [[CrossRef](#)]
20. Zuo, H.; Liu, Q.; Wang, T.; Ma, L.; Zhang, Q.; Zhang, Q. Hydrodeoxygenation of Methyl Palmitate over Supported Ni Catalysts for Diesel-like Fuel Production. *Energy Fuels* **2012**, *26*, 3747–3755. [[CrossRef](#)]
21. Ochoa-Hernández, C.; Yang, Y.; Pizarro, P.; de la Peña O’Shea, V.A.; Coronado, J.M.; Serrano, D.P. Hydrocarbons production through hydrotreating of methyl esters over Ni and Co supported on SBA-15 and Al-SBA-15. *Catal. Today* **2013**, *210*, 81–88. [[CrossRef](#)]
22. Ki Kim, S.; Yoon, D.; Lee, S.-C.; Kim, J. Mo₂C/Graphene Nanocomposite as a Hydrodeoxygenation Catalyst for the Production of Diesel Range Hydrocarbons. *ACS Catal.* **2015**, *5*, 3292–3303. [[CrossRef](#)]
23. Hollak, S.A.W.; Gosselink, R.W.; van Es, D.S.; Bitter, J.H. Comparison of tungsten and molybdenum carbide catalysts for the hydrodeoxygenation of oleic acid. *ACS Catal.* **2013**, *3*, 2837–2844. [[CrossRef](#)]
24. Wang, H.; Yan, S.; Salley, S.O.; Simon Ng, K.Y. Support effects on hydrotreating of soybean oil over NiMo carbide catalyst. *Fuel* **2013**, *111*, 81–87. [[CrossRef](#)]
25. Monnier, J.; Sulimma, H.; Dalai, A.; Caravaggio, G. Hydrodeoxygenation of oleic acid and canola oil over alumina-supported metal nitrides. *Appl. Catal. A Gen.* **2010**, *382*, 176–180. [[CrossRef](#)]
26. Chen, J.; Shi, H.; Li, L.; Li, K. Deoxygenation of methyl laurate as a model compound to hydrocarbons on transition metal phosphide catalysts. *Appl. Catal. B Environ.* **2014**, *144*, 870–884. [[CrossRef](#)]
27. Chen, J.; Yang, Y.; Shi, H.; Li, M.; Chu, Y.; Pan, Z.; Yu, X. Regulating product distribution in deoxygenation of methyl laurate on silica-supported Ni–Mo phosphides: Effect of Ni/Mo ratio. *Fuel* **2014**, *129*, 1–10. [[CrossRef](#)]
28. Shi, H.; Chen, J.; Yang, Y.; Tian, S. Catalytic deoxygenation of methyl laurate as a model compound to hydrocarbons on nickel phosphide catalysts: Remarkable support effect. *Fuel Process. Technol.* **2013**, *116*, 161–170. [[CrossRef](#)]
29. Yang, Y.; Chen, J.; Shi, H. Deoxygenation of Methyl Laurate as a Model Compound to Hydrocarbons on Ni₂P/SiO₂, Ni₂P/MCM-41, and Ni₂P/SBA-15 catalysts with different dispersions. *Energy Fuels* **2013**, *27*, 3400–3409. [[CrossRef](#)]
30. Yang, Y.; Ochoa-Hernández, C.; de la Peña O’Shea, V.A.; Coronado, J.M.; Serrano, D.P. Ni₂P/SBA-15 As a Hydrodeoxygenation Catalyst with Enhanced Selectivity for the Conversion of Methyl Oleate Into n-Octadecane. *ACS Catal.* **2012**, *2*, 592–598. [[CrossRef](#)]
31. Yang, Y.; Ochoa-Hernández, C.; Pizarro, P.; de la Peña O’Shea, V.A.; Coronado, J.M.; Serrano, D.P. Synthesis of Nickel Phosphide Nanorods as Catalyst for the Hydrotreating of Methyl Oleate. *Top. Catal.* **2012**, *55*, 991–998. [[CrossRef](#)]

32. Yang, Y.; Ochoa-Hernández, C.; Pizarro, P.; de la Peña O'Shea, V.A.; Coronado, J.M.; Serrano, D.P. Influence of the Ni/P ratio and metal loading on the performance of Ni₂P/SBA-15 catalysts for the hydrodeoxygenation of methyl oleate. *Fuel* **2015**, *144*, 60–70. [[CrossRef](#)]
33. Zarchin, R.; Rabaev, M.; Vidruk-Nehemya, R.; Landau, M.V.; Herskowitz, M. Hydroprocessing of soybean oil on nickel-phosphide supported catalysts. *Fuel* **2015**, *139*, 684–691. [[CrossRef](#)]
34. Pan, Z.; Wang, R.; Li, M.; Chu, Y.; Chen, J. Deoxygenation of methyl laurate to hydrocarbons on silica-supported Ni-Mo phosphides: Effect of calcination temperatures of precursor. *J. Energy Chem.* **2015**, *24*, 77–86. [[CrossRef](#)]
35. Xue, Y.; Guan, Q.; Li, W. Synthesis of bulk and supported nickel phosphide using microwave radiation for hydrodeoxygenation of methyl palmitate. *RSC Adv.* **2015**, *5*, 53623–53628. [[CrossRef](#)]
36. Zheng, Z.; Li, M.-F.; Chu, Y.; Chen, J.-X. Influence of CS₂ on performance of Ni₂P/SiO₂ for deoxygenation of methyl laurate as a model compound to hydrocarbons: Simultaneous investigation on catalyst deactivation. *Fuel Process. Technol.* **2015**, *134*, 259–269. [[CrossRef](#)]
37. Lee, S.I.; Kim, D.W.; Jeon, H.J.; Ju, S.J.; Ryu, J.W.; Oh, S.H.; Koh, J.H. Metal Phosphorus Compound for Preparing Biodiesel and Method Preparing Biodiesel Using the Same. U.S. Patent US2014/0150332A1, 5 June 2014.
38. Alvarez-Galvan, M.; Campos-Martin, J.; Fierro, J. Transition Metal Phosphides for the Catalytic Hydrodeoxygenation of Waste Oils into Green Diesel. *Catalysts* **2019**, *9*, 293. [[CrossRef](#)]
39. Deliy, I.; Shamanaev, I.; Gerasimov, E.; Pakharukova, V.; Yakovlev, I.; Lapina, O.; Aleksandrov, P.; Bukhtiyarova, G. HDO of Methyl Palmitate over Silica-Supported Ni Phosphides: Insight into Ni/P Effect. *Catalysts* **2017**, *7*, 298. [[CrossRef](#)]
40. Shamanaev, I.V.; Deliy, I.V.; Aleksandrov, P.V.; Gerasimov, E.Y.; Pakharukova, V.P.; Kodenev, E.G.; Ayupov, A.B.; Andreev, A.S.; Lapina, O.B.; Bukhtiyarova, G.A. Effect of precursor on the catalytic properties of Ni₂P/SiO₂ in methyl palmitate hydrodeoxygenation. *RSC Adv.* **2016**, *6*, 30372–30383. [[CrossRef](#)]
41. He, L.; Wu, C.; Cheng, H.; Yu, Y.; Zhao, F. Highly selective and efficient catalytic conversion of ethyl stearate into liquid hydrocarbons over a Ru/TiO₂ catalyst under mild conditions. *Catal. Sci. Technol.* **2012**, *2*, 1328. [[CrossRef](#)]
42. Shamanaev, I.; Aleksandrov, P.; Kodenev, E.; Pakharukova, V.; Gerasimov, E.; Deliy, I.; Bukhtiyarova, G. Synergetic Effect of Ni₂P/SiO₂ and γ-Al₂O₃ Physical Mixture in Hydrodeoxygenation of Methyl Palmitate. *Catalysts* **2017**, *7*, 329. [[CrossRef](#)]
43. Deliy, I.; Shamanaev, I.; Aleksandrov, P.; Gerasimov, E.; Pakharukova, V.; Kodenev, E.; Yakovlev, I.; Lapina, O.; Bukhtiyarova, G. Support Effect on the Performance of Ni₂P Catalysts in the Hydrodeoxygenation of Methyl Palmitate. *Catalysts* **2018**, *8*, 515. [[CrossRef](#)]
44. Laurent, E.; Delmon, B. Influence of water in the deactivation of a sulfided NiMo₂-Al₂O₃ catalyst during hydrodeoxygenation. *J. Catal.* **1994**, *146*, 281–291. [[CrossRef](#)]
45. Şenol, O.İ.; Viljava, T.-R.; Krause, A.O.I. Hydrodeoxygenation of methyl esters on sulphided NiMo/γ-Al₂O₃ and CoMo/γ-Al₂O₃ catalysts. *Catal. Today* **2005**, *100*, 331–335. [[CrossRef](#)]
46. Shamanaev, I.V.; Deliy, I.V.; Aleksandrov, P.V.; Reshetnikov, S.I.; Bukhtiyarova, G.A. Methyl palmitate hydrodeoxygenation over silica-supported nickel phosphide catalysts in flow reactor: Experimental and kinetic study. *J. Chem. Technol. Biotechnol.* **2019**. [[CrossRef](#)]
47. Prins, R.; Bussell, M.E. Metal Phosphides: Preparation, Characterization and Catalytic Reactivity. *Catal. Lett.* **2012**, *142*, 1413–1436. [[CrossRef](#)]
48. Liu, X.; Xu, L.; Zhang, B. Essential elucidation for preparation of supported nickel phosphide upon nickel phosphate precursor. *J. Solid State Chem.* **2014**, *212*, 13–22. [[CrossRef](#)]
49. Peroni, M.; Mancino, G.; Baráth, E.; Gutiérrez, O.Y.; Lercher, J.A. Bulk and γ-Al₂O₃ supported Ni₂P and MoP for hydrodeoxygenation of palmitic acid. *Appl. Catal. B Environ.* **2016**, *180*, 301–311. [[CrossRef](#)]
50. Li, K.; Wang, R.; Chen, J. Hydrodeoxygenation of Anisole over Silica-Supported Ni₂P, MoP, and NiMoP Catalysts. *Energy Fuels* **2011**, *25*, 854–863. [[CrossRef](#)]
51. Bui, P.; Cecilia, J.A.; Oyama, S.T.; Takagaki, A.; Infantes-Molina, A.; Zhao, H.; Li, D.; Rodríguez-Castellón, E.; Jiménez López, A. Studies of the synthesis of transition metal phosphides and their activity in the hydrodeoxygenation of a biofuel model compound. *J. Catal.* **2012**, *294*, 184–198. [[CrossRef](#)]

52. Montesinos-Castellanos, A.; Zepeda, T.A.; Pawelec, B.; Fierro, J.L.G.; De Los Reyes, J.A. Preparation, characterization, and performance of alumina-supported nanostructured Mo-phosphide systems. *Chem. Mater.* **2007**, *19*, 5627–5636. [[CrossRef](#)]
53. Newsam, J.M.; Treacy, M.M.J.; Koetsier, W.T.; Gruyter, C.B.D. Structural Characterization of Zeolite Beta. *Proc. R. Soc. A Math. Phys. Eng. Sci.* **1988**, *420*, 375–405. [[CrossRef](#)]
54. Flanigen, E.M.; Lok, B.M.; Patton, R.L.; Wilson, S.T. Aluminophosphate molecular sieves and the periodic table. *Pure Appl. Chem.* **1986**, *58*, 1351–1358. [[CrossRef](#)]
55. Peroni, M.; Lee, I.; Huang, X.; Baráth, E.; Gutiérrez, O.Y.; Lercher, J.A. Deoxygenation of Palmitic Acid on Unsupported Transition-Metal Phosphides. *ACS Catal.* **2017**, *7*, 6331–6341. [[CrossRef](#)]
56. Gosselink, R.W.; Hollak, S.A.W.; Chang, S.W.; Van Haveren, J.; De Jong, K.P.; Bitter, J.H.; van Es, D.S. Reaction pathways for the deoxygenation of vegetable oils and related model compounds. *ChemSusChem* **2013**, *6*, 1576–1594. [[CrossRef](#)] [[PubMed](#)]
57. File, P.D. *JCPDS—International Centre for Diffraction Data; ICDD: Swarthmore, PA, USA, 1997.*



© 2019 by the authors. Licensee MDPI, Basel, Switzerland. This article is an open access article distributed under the terms and conditions of the Creative Commons Attribution (CC BY) license (<http://creativecommons.org/licenses/by/4.0/>).